Available online at www.sciencedirect.com
ScienceDirect
Journal of Nuclear Materials 367–370 (2007) 97–101
journal of nuclear materials
www.elsevier.com/locate/jnucmat

Research and development on the China low activation martensitic steel (CLAM) ☆

Jinnan Yu [a,*], Qunying Huang [b], Farong Wan [c]

[a] China Institute of Atomic Energy, P.O. Box 275-51, Beijing 102413, China
[b] Institute of Plasma Physics, CAS, P.O. Box 1126, Hefei, Anhui 230031, China
[c] Department of Material Physics and Chemistry, University of Science and Technology, Beijing 100083, China

Abstract

Chinese low activation martensitic steel (CLAM) has been designed with improved composition, and its performance, such as tensile properties, ductile–brittle transition temperature ($DBTT_{41J}$), creep and thermal physical properties, has been determined. The interaction experiments between CLAM and plasma were carried out in the HT-7 tokamak facility and the activities, afterheat and gamma dose rate for CLAM as a function of cooling time (CT) were calculated to obtain the required control levels of impurities in CLAM. The insulator coatings on CLAM steel prepared by the CVD process at 700 °C and 740 °C have pure Al_2O_3 and Al_2O_3 with an oxygen deficiency layer on surface about 1 μm thick. The electrical resistivity of the coating reaches about $10^4\ \Omega m^2$ on the surface.

1. Introduction

The current international fusion strategy is designed to demonstrate the scientific feasibility and economic and environmental attractiveness of magnetic fusion energy within ~35 years [1–6]. Advances in plasma physics and radiation-resistant materials would set the stage for design and construction of a demonstration power plant (Demo) within about 30 years. The worldwide fusion materials programs have a strong emphasis on structural materials R&D because reduced activation structural materials are key to reaching fusion's potential as a technologically viable energy source with no long-lived radioactive waste and no risk of severe accidents that would require widespread public evacuation. Austenitic steel is appropriate for devices like ITER with a moderate upper temperature and limited neutron fluence, but they are very sensitive to He-induced high temperature embrittlement and its compatibility with Li and LiPb is relatively low. In addition, the attempts to replace Ni by Mn for decreasing the high long-term radioactivity have not been successful [7]. They have limited potential for a future breeding blanket.

Reduced activation ferritic/martensitic (RAFM) steel has good thermal conductivity, low thermal expansion coefficient, good resistance to radiation-induced swelling and helium embrittlement, good compatibility with a wide range of gaseous and

☆ This work is supported by Chinese National Natural Science Foundation with grant number 10375067.
* Corresponding author. Tel.: +86 10 69357232; fax: +86 10 69357008.
E-mail address: yujn@iris.ciae.ac.cn (J. Yu).

0022-3115/$ - see front matter © 2007 Elsevier B.V. All rights reserved.
doi:10.1016/j.jnucmat.2007.03.236

liquid coolants. Their compatibility with liquid metal (Pb–Li) up to 480 °C offers the potential for low activation systems but formidable challenges still exist. A reduced activation 9Cr ferritic martensitic steel, called Eurofer has been accepted as the basic structural material in EU DEMO design and will be used as structural material in the two EU test blanket modules (TBM) to be installed in ITER [7].

Based on the progress of RAFM steel research, CLAM steel has been designed with improvement composition, and their performance has been determined to be comparable to 9Cr–2WVTa [10] and Eurofer97 [5] steels. The thermal physical properties have also been measured and are given in this paper. The data indicate that CLAM can be used as a leading candidate for the structural materials in the two Blanket to be tested in ITER.

The key unsolved issues include the effect of irradiation on fracture properties (particularly at low temperature) and the role of transmutation helium on the deformation and fracture of irradiated materials at low and high temperatures. Optimized coolant inlet temperature and coolant flow schemes are envisaged to use the full temperature window of CLAM steel from 300 to 500 °C. The lower limit is dictated by irradiation embrittlement, and the upper limit is basically given by long-term mechanical properties such as creep rupture and fatigue–creep interaction, but also by a reduction in static mechanical properties.

2. Composition, structure and tensile properties

The composition of CLAM steel has been designed to improve the performance, such as changing tungsten content to 1.5% to decrease the amount of Laves phase precipitation in weld metal and heat-affected zone at 550 °C [8,9]. Tantalum content was increased to 0.15% to have a smaller prior-austenite grain size and small spherical Ta-rich precipitate (TaC) to increase strength, as well as to increase the creep strength [10–12]. Adding a suitable amount of manganese is to improve the compatibility with LiPb liquid and suitable Si is to improve the welding behavior. Several 5 kg ingot castings of CLAM steel produced by a vacuum induction melting furnace with highly purified raw materials have been hot-forged to square rods (13×13 mm) and normalized at 980 °C for 30 min followed by water quenching to obtain a martensitic microstructure. This was followed tempering at 760 °C for 90 min followed by air-cooling. The chemical composition of CLAM and reference materials is shown in Table 1.

The carbon content is 0.11%, which marks the transition from ferritic steel structure (bcc, cubic) to the martensitic steel structure (bcc, rectangular) after quenching. The hardness of the martensitic steel with this content of carbon is high enough to be comparable to the hardening contributed by the radiation-induced defect clusters for the martensitic steel under irradiation. Therefore, the increase of yield stress under irradiation is much less than that of ferritic steel with low carbon content. The ultimate stress is insensitive to irradiation. Thus, the DBTT shift under irradiation for martensitic steel is much less than that for ferritic steel, so long as the correct composition is selected.

The 9Cr alloy class exhibited the smallest increases in hardening under irradiation, which has a minimum DBTT shift under irradiation [13,14]. At 550 °C for materials with $W \geqslant 2\%$, the precipitation of Laves phase and the segregation of W at grain boundary occur [8,9]. The tungsten content of CLAM is 1.5%, which decreases the amount of Laves phase precipitation in weld metal and heat-affected zone at 550 °C. But the tungsten content of CLAM is a little larger than that of Eurofer97, because adding tungsten improves the DBTT and is used for tempering resistance, as well as increasing the creep strength. Tantalum content increases to 0.15% reduce the prior-austenite grain size and form small spherical Ta-rich precipitates (TaC) to increase strength, as well as increasing the creep strength. Adding suitable amount of manganese improves the compatibility with LiPb liquid and Si addition improves the welding behavior.

Table 1
Chemical composition of China low activation martensitic steel (CLAM) and other RAM steels

Kind of steel	Fe	Cr	W	C	V	Ta	Mn	Si	N
CLAM	Bal.	8.98	1.55	0.11	0.21	0.15	0.40	0.01	0.02
Eurofer97	Bal.	8.82	1.1	0.10	0.19	0.068	0.37	0.005	0.021
9Cr–2WVTa	Bal.	8.90	2.01	0.11	0.23	0.06	0.44	0.21	0.021
JLF-1	Bal.	8.87	1.9	0.10	0.19	0.084	0.48	0.24	0.0244

Table 2
Yield strength, ultimate strength and elongation of CLAM (HEAT0311A)

Test temperature	Kind of steel	Yield strength (0.2% offset) (MPa)	Ultimate strength (MPa)	Uniform elongation (%)	Total elongation (%)
Room temperature	CLAM	486.8 ± 18.69	629.0 ± 21.44	8.4 ± 0.65	25.1 ± 0.38
	JFL-1	514	628		24
350 °C	CLAM	423.0 ± 8.35	513.0 ± 5.05	4.9 ± 0.35	18.6 ± 0.25
400 °C	JFL-1	363	465		16

Ref. [15].

Metallographic analysis of CLAM indicates that the mean intercept is 2.7 μm, the fraction of grains with a size number from 10 to 11.5 is 63.36% and the mean grain size is 3.5 μm in diameter. The tensile properties are shown in Table 2 [15], which are comparable to 9Cr–2WVTa [10] and Eurofer97 steels [5]. The further efforts will make the grain size of CLAM more refined to improve CLAM performance.

3. Impact toughness, ductile–brittle transition temperature ($DBTT_{41J}$) and creep properties

Standard V-notch impact tests have been carried out on CLAM specimen. Impact toughness and the ductile to brittle transition temperature (DBTT) are shown in Fig. 1. The DBTT for an absorbed energy of 41 J is −95 °C and that for 68 J is −91 °C. The lateral expansion transition temperature curve shows the transition temperature for 0.89 mm lateral expansion to be −91 °C.

Images of the fracture surface of an impact specimen tested at −98 °C from a scanning electron microscope (SEM) observation are shown in Fig. 2. Sites located 0.7 mm, 1.9 mm and 3.3 mm distance from V-notch are shown in Fig. 2(a)–(c), respectively. Fig. 2(a) shows grain deformation, originating from the plastic structure. Fig. 2(c) shows no grain deformation, indicating a brittle structure. But, in Fig. 2(b), some grains near the notch direction have light deformation and the others have no deformation. This indicates that the fracture is in the ductile to brittle transition, even at the temperature −98 °C. Some micro-cracks are formed at the surface of the notch during the early part of the impact test and grow during the impact process, indicating a ductile process. When one largest crack reaches a critical size, the main crack propagates with sonic speed and governs the whole fracture process in a brittle manner.

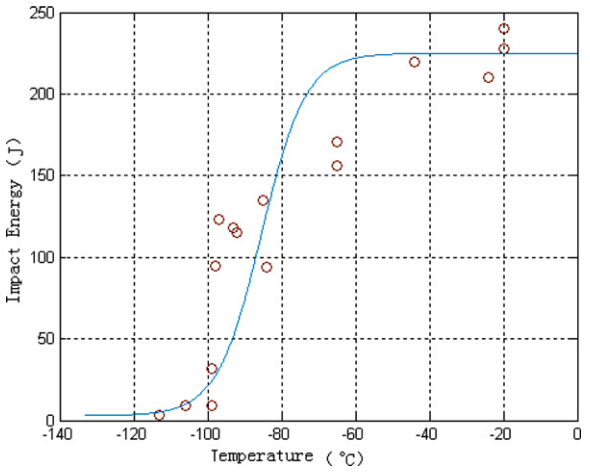

Fig. 1. Absorbed impact energy to transition temperature curve of CLAM products, $T_{41J} = -95$ °C; $T_{68J} = -91$ °C.

The creep test has been carried out in the fusion materials technology group of CRPP. The curve of creep strain as a function of time at 550 °C with 250 MPa stress is shown in Fig. 3. The creep rate of CLAM is less than that of Eurofer97, but the rupture time is less than that of Eurofer97. This indicates that CLAM steel has better creep strength than Eurofer97 and the elongation is less than that of Eurofer97. If CLAM steel is improved with smaller grain size, the elongation should improve and the rupture time will increase.

4. The interaction with plasma [16]

The CLAM and Eurofer97 specimens were exposed on the scrape off layer of a plasma located at 0.29 m (position 1) and 0.30 m (position 2) from the center of the plasma in the HT-7 tokamak facility. HT-7 is a medium size tokamak the major radius $R = 1.22$ m, minor radius $a = 0.285$ m, elongation $\kappa < 1.3$, toroidal magnetic field $B_t < 2.5$ T, $n_e < 6 \times 10^{13}$ cm^{-3}, $T_e < 2$ keV, $T_i < 0.6$ keV. For our experiments [16] the operating parameters are the following: $R = 1.22$ m, $a = 0.27$ m, $n_e = 1.5 \times 10^{13}$ cm^{-3}, $T_e = 700$ eV, $T_i = 450$ eV. The specimens

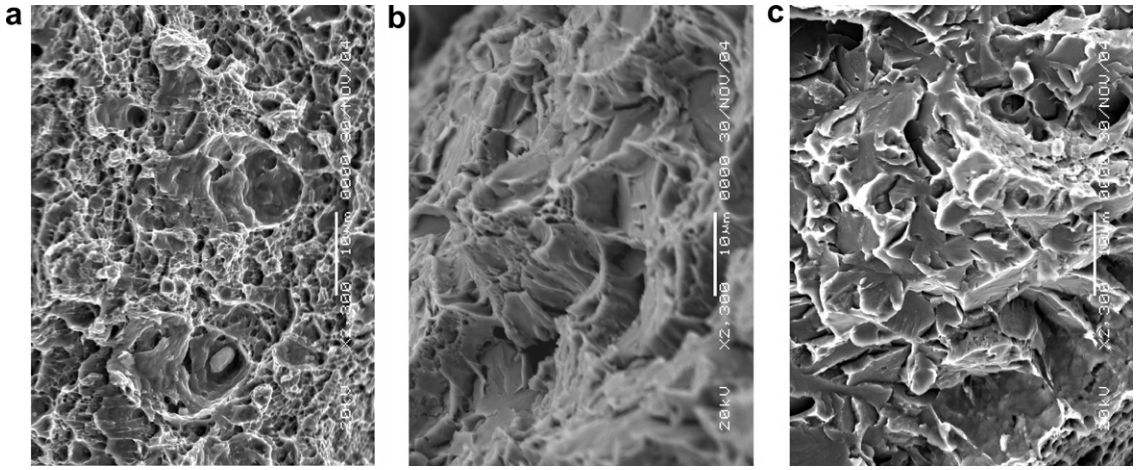

Fig. 2. SEM images on the fractured surface site located 0.7 mm, 1.9 mm and 3.3 mm from the V-notch distance in figures a, b and c, respectively, the impact testing temperature at −98 °C.

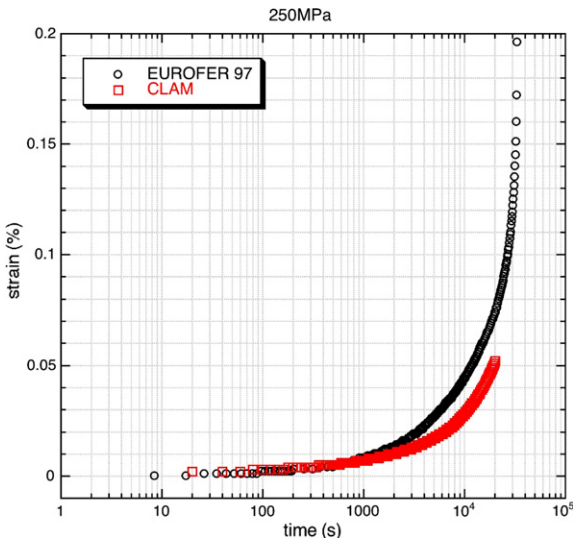

Fig. 3. The creep strain of CLAM with time at 550 °C with 250 MPa stress.

were irradiated for 802 shots with a hydrogen and deuterium discharge; the average duration time for each shot $\tau = 1500$ ms. The electron and ion density n_e, electron and ion temperature T_e, T_i at site 1 are about $1.5 \times 10^{12}\,\mathrm{cm}^{-3}$, 60 eV and 35 eV, respectively. The values at site 2 are about $0.5 \times 10^{12}\,\mathrm{cm}^{-3}$, 38 eV and 20 eV. The results indicate that a threshold ion energy and threshold fluence exist to induce a blister. The blistering for the CLAM specimen at site 1 is more than that of Eurofer97, but the results at site 2 are reversed, i.e. the surface of CLAM specimen is much smoother than that of Eurofer97. This also shows that CLAM steel is harder than Eurofer97, because of more tungsten and tantalum.

5. Insulator coating on CLAM and Eurofer97 steel [17]

An Al based coating on CLAM and Eurofer97 steel was made by the CVD process at 700 °C and 740 °C. After coating, the clean specimens were oxidized in 0.133 Pa oxygen atmosphere at 700 °C and 740 °C to form the Al_2O_3 layer on the surface. The typical thickness of the aluminized layer is 20 μm, including the 10 μm thick external layer and a 10 μm thick internal layer. The thickness of the Al_2O_3 layer is about 1 μm. The microstructure, micro-hardness profile, composition depth dependence and electrical resistivity of the coating layer were measured. The coatings on CLAM steel have higher micro-hardness and are denser than those on Eurofer97 steel with the CVD process at 740 °C. The Al_2O_3 layer with CVD process at 700 °C has higher micro-hardness and is denser than that for 740 °C. The coating surface analysis by the XPS method indicated that the coating on the surface is Al_2O_3. The layer consists of pure Al_2O_3 and Al_2O_3 with oxygen deficiency in a 10 nm thick layer near the surface.

6. Thermal physics properties

The thermal conductivity, thermal expansion coefficient and thermal capacity have been measured as shown in Table 3. The measurement error for thermal capacity, thermal expansion coefficient

Table 3
Thermal capacity, thermal expansion coefficient and thermal conductivity

Temperature °C	Thermal capacity (J/g °C)	Thermal expansion coefficient (10^{-6} °C)	Thermal conductivity (J/s cm °C)
25			0.265
100	0.48		0.256
200			0.242
300	0.52		0.229
350		12.04	
400		12.06	0.216
450		12.16	
500	0.55	12.18	0.202
550		12.28	
600			0.189

and thermal conductivity is 2%, 1.26% and 3%, respectively.

7. Analysis on activation of CLAM steel [18]

Activities, afterheats and gamma dose rates for RAFM steels with cooling time (CT) were calculated using the FISPACT inventory code with FENDL/A-2 data library based on the first wall (FW) neutron spectrum of the fusion-driven subcritical system (FDS) from the Monte Carlo transport code MCNP/4C calculation with FENDL-2 data library [18]. There is almost no difference in total activation values between CLAM and other RAFM steels for short CT. The difference between them becomes larger with longer CT. That is mainly because the dominant nuclides contributing to activation levels for shorter CT are products from the activation of main elements of the steels, which are quite similar for all the RAFM steels. However, the dominant nuclides for longer CT are products from activation of impurities, which are quite different among these steels. The dose rates of the RAFM steels reduce to remote handling level when CT is ~50 years for F82H and JLF-1, 67 years for CLAM and Eurofer97 and longer than 100 years for 9Cr–2WVTa. None of these steels reduce to the hands-on recycling level during CT less than 10^4 years.

Short-lived nuclides ^{60}Co and ^{55}Fe dominate the total dose rate of CLAM steel to a CT of ~70 and 35 years, respectively. Afterwards, the long-lived nuclide ^{94}Nb becomes the dominant nuclide to the total dose rate of CLAM steel.

8. Summary

China low activation martensitic steel has been designed to improve their composition and their performance has been determined, which are similar to Eurofer97. The creep rate and the rupture time of CLAM are less than that of Eurofer97, because CLAM steel is harder than Eurofer97. The thermal physical properties of CLAM steel have been measured and are good enough to be used in engineering design.

The experiments of plasma interaction with CLAM and Eurofer97 specimens in the scrape off layer of a plasma indicate that blistering of CLAM specimens is more than Eurofer97 in the intense plasma region and much less than Eurofer97 in the less intense region of the plasma, because CLAM steel is harder than Eurofer97.

The pure Al_2O_3 coatings on CLAM steel and calculation on activation of CLAM steel have been done.

References

[1] E.E. Bloom, S.J. Zinkle, F.W. Wiffen, J. Nucl. Mater. 329–333 (2004) 12.
[2] K. Lackner, R. Andreani, D. Campbell, et al., J. Nucl. Mater. 307–311 (2002) 10.
[3] Y. Wu, Fusion Eng. Des. 63&64 (2002) 73.
[4] Y. Wu, FDS Team, Fusion Eng. Des. 81 (2006) 2713.
[5] T. Muroga, M. Gasparotto, S.J. Zinkle, Fusion Eng. Des. 61&62 (2002) 13.
[6] R. Goldston et al., J. Fus. Energy 21 (2002) 61.
[7] R. Andreani, E. Diegele, R. Laesser, et al., J. Nucl. Mater. 329–333 (2004) 20.
[8] T. Sawai, K. Shiba, A. Hishinuma, J. Nucl. Mater. 283–287 (2000) 657.
[9] J. Lapena, M. Garcia-Mazario, P. Fernandez, et al., J. Nucl. Mater. 283–287 (2000) 662.
[10] T. Hasegawa et al., J. Nucl. Mater. 258–263 (1998) 1153.
[11] A. Alamo et al., J. Nucl. Mater. 258–263 (1998) 1229.
[12] Y. de Carlan, A. Alamo, M.H. Mathon, et al., J. Nucl. Mater. 283–287 (2000) 672.
[13] A. Kohyama, A. Hishinuma, D.S. Gelles, et al., J. Nucl. Mater. 233–237 (1996) 138.
[14] M. Rieth, B. Dafferner, H.D. Rohrig, J. Nucl. Mater. 233–237 (1996) 351.
[15] Y. Li, Q. Huang, Y. WU, et al., J. Nucl. Mater., these Proceedings, doi:10.1016/j.jnucmat.2007.03.012.
[16] Q. Li, Q. Huang, J. Yu, et al., Chinese J. Nucl. Sci. Eng. 24 (2004) 157.
[17] X. Li, G. Yu, J. Yu, et al., J. Nucl. Mater. 329–333 (2004) 1407.
[18] Q. Huang, J. Li, Y. Chen, J. Nucl. Mater. 329–333 (2004) 268.